FULL PAPER

Cationic Decamethylbimetallocenes of Cobalt and Nickel: Synthesis, Redox Behavior and Magnetic Interaction

Peter Hudeczek,[a] Frank H. Köhler,*[a] Pierre Bergerat,[b] and Olivier Kahn*[b]

Dedicated to Professor Ernst Otto Fischer on the occasion of his 80th birthday

Abstract: Stepwise oxidation of deca-methylbinickelocene ([Ni′Ni′]) with decamethylferrocenium hexafluoro-phosphate has produced $[Ni′Ni′]^+[PF_6]^-$ and $[Ni′Ni′]^{2+}[PF_6]_2^-$ in yields of up to 78 %. $[Co′Co′]^+[PF_6]^-$ has been synthesized almost quantitatively by reduction of $[Co′Co′]^{2+}[PF_6]_2^-$ with sodium amalgam. These solid salts are stable in the absence of wet air. In acetone solution the nickel derivatives decompose very slowly to give $[Cp_2^*Ni]^+$ (Cp* = penta-methylcyclopentadienyl) and other un-known paramagnetic species. The Cp* ligands of $[Co′Co′]^+$ have been deuter-ated selectively by prolonged exposure to CD_3CN. The synthetic work is based on cyclic voltammetry (CV) studies. A double set of half-wave potentials was obtained for each dinuclear compound [M′M′] (M = Fe, Co, Ni); these were compared with those of [Cp*MCp] species. The first oxidation in [M′M′] occurs at lower potential (with one exception) than in [Cp*MCp], while the second is higher; potential separations of up to 0.86 V have been found. NMR experi-ments indicate delocalization in the mixed-valence cations $[Co′Co′]^+$ and $[Ni′Ni′]^+$, with the intra-cation electron transfer faster than $5 \times 10^4\ s^{-1}$. Magnetic studies suggest that the valencies of solid $[Ni′Ni′]^+[PF_6]^-$ are localized. While $[Co′Co′]^+[PF_6]^-$ is a simple para-magnet ($S = 1/2$), $[Ni′Ni′]^+[PF_6]^-$ and $[Ni′Ni′]^{2+}[PF_6]_2^-$ show weak ($J = -11.8\ cm^{-1}$; $\mathbf{H} = -J\mathbf{S}_A \cdot \mathbf{S}_B$) and strong ($J = -240\ cm^{-1}$) antiferromagnetic in-teractions, respectively. $[Ni′Ni′]^+[PF_6]^-$ undergoes a reversible magnetic phase transition, and tends to ferromagnetic interaction below 14 K. This magnetic interaction is promoted by the bridging fulvalene ligand, which carries appreci-able spin. The ^1H and ^{13}C NMR spectra reflect the magnetic behavior and con-firm the structure. Through comparison of the experimental signal patterns with theoretical patterns (based on extended Hückel calculations) it was possible to determine which MOs are involved in the spin delocalization.

Keywords: cobalt · magnetic prop-erties · mixed-valence compounds · nickel · sandwich complexes

Introduction

A one-bond ligand bridge is one of the simplest ways of linking transition metal centers; the coupling of two cyclo-pentadienyls (Cp) to form the fulvalenediyl ligand is a well-known example. The bi- and polymetallic derivatives of this ligand have received much attention, as the various kinds of interactions between the metal centers can relate fulvalene compounds to molecular electronics. Many such interactions involve electron transfers (ETs) as outlined by Astruc,[1] who also recently summarized his enlightening work on electronic

communication across fulvalene- and biphenyl-type ligands.[2] A particularly well-studied case is that of linked metallocenes, which have been reviewed in detail by Barlow and O'Hare.[3] Their survey illustrated that most studies have concerned either ferrocenes or, in the case of the fulvalenediyl ligand, biferrocenes.

With cationic biferrocenes almost all efforts have been devoted to the paramagnetic (spin $S = 1/2$) mixed-valence monocations. The groups of both Hendrickson[4a] and Dong,[4b] amongst others, have shown that the valencies may be readily trapped or detrapped (delocalized) by changing the substituents and/or the counterions. Reports on paramagnetic bimetallocenes containing metals other than iron are scarce,[5] and before we started work on such non-ferrous bimetallo-cenes,[6] only the bicobaltocene monocation had been de-scribed.[4a] In the course of detailed investigations we found that the neutral decamethylbimetallocenes ([M′M′])[7] display strikingly different magnetic interactions, which range from weakly antiferromagnetic to strongly ferromagnetic.[8] This prompted us to study also the cationic decamethylbimetallo-cenes ([M′M′]$^{n+}$, M = Co, Ni) with emphasis on their magnetic behavior and on the distribution of the unpaired electron spin.

[a] Prof. Dr. F. H. Köhler, Dr. P. Hudeczek
Anorganisch-chemisches Institut
Technische Universität München, D-85747 Garching (Germany)
Fax: (+49) 89-2891-3109
E-mail: f.h.koehler@lrz.tu-muenchen.de

[b] Prof. O. Kahn, Dr. P. Bergerat
Laboratoire des Sciences Moléculaires
ICMCB, UPR 9048 du CNRS
F-33608 Pessac Cédex (France)
Fax: (+33) 556-842-649
E-mail: kahn@icmcb.u-bordeaux.fr

Results

Synthesis and redox behavior: For the parent complex biferrocene, it was found over twenty-five years ago that the electron transfers (ETs) which yield its mono- and dications are well separated (0.35 V in CH_3CN),[9] and that both species can indeed be isolated.[10] Since the corresponding binickelocene ([NiNi]) proved to be unstable, we synthesized the decamethyl derivative as part of the series [M′M′] (M = V, Fe, Co, Ni, and—less well characterized—Cr)[8] and subsequently recorded the cyclic voltammograms (CV) of [Fe′Fe′], [CoCo], and [Ni′Ni′].[6b] The CVs of [Fe′Fe′] and [Co′Co′] were obtained independently by Astruc,[11a] who has also studied in detail the cations [Fe′Fe′]+ [11b] and [Fe′Fe′]2+.[11c]

The CV results are summarized in Figure 1. It is useful to compare the ETs of [M′M′] to those of [Cp*MCp] ([M′]),[7] because, formally, the coupling of two sandwiches [M′] yields [M′M′]. Such coupling is accompanied by stepwise one-

Abstract in German: *Durch schrittweise Oxidation von Decamethylbinickelocen ([Ni′Ni′]) mit Decamethylferroceniumhexafluorophosphat wurden [Ni′Ni′]+[PF₆]⁻ und [Ni′Ni′]²⁺[PF₆]₂⁻ in Ausbeuten von bis zu 78 % erhalten. [Co′Co′]+[PF₆]⁻ wurde fast quantitativ durch Reduktion von [Co′Co′]²⁺[PF₆]₂⁻ mit Natriumamalgam synthetisiert. Die festen Salze waren unter Ausschluß von feuchter Luft stabil. In Aceton zersetzten sich die Nickelderivate sehr langsam unter Bildung von [Cp₂*Ni]+ (Cp* = Pentamethylcyclopentadienyl) sowie anderen unbekannten paramagnetischen Spezies, und die Cp*-Liganden von [Co′Co′]+ wurden durch längeres Stehen in CD₃CN selektiv deuteriert.*

*Die synthetischen Arbeiten bauten auf cyclovoltammetrischen Untersuchungen auf. Im Vergleich mit [Cp*MCp] (M = Fe, Co, Ni) wurde ein doppelter Satz von Halbstufenpotentialen für die zweikernigen Verbindungen [M′M′] gefunden. Die erste Oxidation erfolgte bei niedrigerem Potential (mit einer Ausnahme) als im Fall von [Cp*MCp], während das zweite Potential höher lag; die Potentialabstände betrugen bis zu 0.86 V. Die gemischtvalenten Kationen [Co′Co′]+ und [Ni′Ni′]+ waren aus Sicht der NMR-Spektroskopie delokalisiert, und der kationeninterne Elektronentransfer war schneller als 5 × 10⁴ s⁻¹. Den Magnetismusmessungen zufolge sind die Valenzen von festem [Ni′Ni′]+[PF₆]⁻ lokalisiert. Während [Co′Co′]+[PF₆]⁻ ein einfaches paramagnetisches Molekül mit S = ¹/₂ ist, wies [Ni′Ni′]+[PF₆]⁻ schwache (J = −11.8 cm⁻¹; **H** = −J**S**ₐ·**S**ᵦ) und [Ni′Ni′]²⁺[PF₆]₂⁻ starke (J = −240 cm⁻¹) antiferromagnetische Wechselwirkungen auf. [Ni′Ni′]+[PF₆]⁻ durchlief einen reversiblen magnetischen Phasentransfer und wies unterhalb von 14 K ferromagnetische Wechselwirkungen auf. Die magnetische Wechselwirkung wird durch den verbrückenden Fulvalenliganden vermittelt, der nennenswerte Spindichte trägt. Die ¹H- und ¹³C-NMR-Spektren spiegelten das magnetische Verhalten wider und bestätigten die Struktur. Der Vergleich der experimentellen Signalmuster mit theoretischen Mustern, die auf Extended-Hückel-Rechnungen basierten, ermöglichte die Bestimmung derjenigen MOs, die an der Spin-Delokalisierung beteiligt sind.*
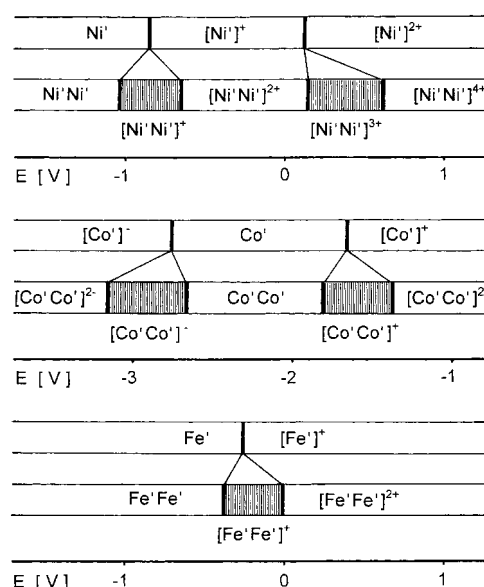

Figure 1. Comparison of the $E_{1/2}$ values for the decamethylbimetallocenes ([M′M′])[7b] with those for [Cp*MCp] ([M′]) (Table 2). All scales are reported in V relative to [Cp₂Fe]/[Cp₂Fe]+. Areas showing the stability range of the mixed-valence ions are hatched.

electron ETs (with separations up to 0.86 eV) rather than by two-electron ETs, as found in biferrocene.[9] The reason is that generation of [M′M′]+ is easier than that of [M′]+ owing to electron delocalization in [M′M′]+, while further oxidation to [M′M′]²⁺ is more difficult because of mainly Coulombic interactions between the two charges. In the light of these results it is surprising that it has been claimed that the parent compound [NiNi][7] undergoes two two-electron ETs to the di- and tetracations rather than being oxidized in four well-separated steps.[5c] This may be linked with the discrepancies in magnetic properties: [NiNi] obtained from fulvalenediid and [Cp₃Ni₂⁺] was reported to be diamagnetic,[5c] whereas antiferromagnetic interaction has been found for [NiNi] and [Ni′Ni′] when synthesized from fulvalenediid and [CpNi{P(OCH₃)₃}] or [Cp*Ni(acac)], respectively.[8]

The CV results of Figure 1 suggested that not only [M′M′]²⁺ but also the monocations should be isolable, as the separation of the $E_{1/2}$ values was rather large (≥375 mV) and, therefore, the tendency of [M′M′]+ to disproportionate was negligible. As shown in Scheme 1 the paramagnetic cations were obtained in 76–97 % yield by reduction of [Co′Co′]²⁺ with sodium amalgam, and by stepwise oxidation of [Ni′Ni′] with [Cp₂*Fe]+[PF₆]⁻. In order to isolate the monocations, the stoichiometry was chosen such that some [M′M′], as well as [M′M′]+, was present. [M′M′] could be removed easily by extraction into hexane. All these new cations are air-sensitive and green to dark green solids which are soluble in acetone, THF, and CH_3CN. The purity of the compounds was checked by full elemental analyses.

Magnetic susceptibility: The magnetic susceptibility data for both [Ni′Ni′]²⁺ and [Ni′Ni′]+ compounds are presented in Figure 2 in the form of a $\chi_m T$ versus T plot (χ_m = zero-field molar magnetic susceptibility, T = temperature).
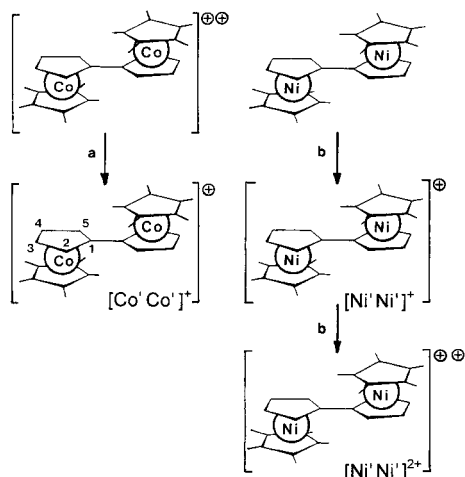
Scheme 1. Routes to paramagnetic decamethylbimetallocenium ions: a) Na/Hg, THF; b) $[Cp_2^*Fe]^+[PF_6]^-$, THF.

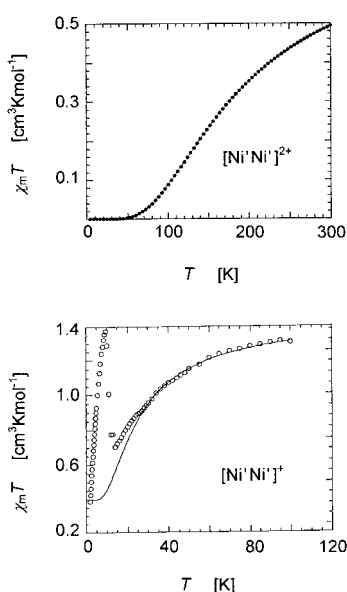Figure 2. $\chi_m T$ versus T curves of $[Ni'Ni']^+[PF_6]^-$ and $[Ni'Ni']^{2+}[PF_6]_2^-$. The best-fit curves are depicted by solid lines.

For $[Ni'Ni']^{2+}$, $\chi_m T = 0.38$ cm³ K mol⁻¹ at room temperature, which is much less than expected for two isolated local spins of $S_{Ni^{III}} = 1/2$. This value decreases very rapidly as T is lowered, and the compound becomes diamagnetic below ca. 60 K. The χ_m versus T curve shows a rounded maximum at about 210 K, characteristic of a strong antiferromagnetic interaction between a singlet ground state and a low-lying triplet excited state. The data can be fitted to the theoretical expression of χ_m valid for a pair of local doublets which leads to a singlet–triplet energy gap of $J = -240$ cm⁻¹ and a Zeeman factor of $g = 2.07$.

The magnetic susceptibility data for the mixed-valence compound $[Ni'Ni']^+$ $[PF_6]^-$ (local spins: $S_{Ni^{III}} = 1/2$ and $S_{Ni^{II}} = 1$) are much more surprising. At room temperature $\chi_m T = 1.3$ cm³ K mol⁻¹, which corresponds approximately to what is expected for isolated local spins $S_{Ni^{III}} = 1/2$ and $S_{Ni^{II}} = 1$. (For delocalized species $\chi_m T$ should be about 0.5 cm³ K mol⁻¹ larger.) As T is lowered, $\chi_m T$ decreases more and more

rapidly, and reaches a value of 0.7 cm³ K mol⁻¹ at 14 K. Further cooling of the sample results initially in an abrupt increase of $\chi_m T$ which shows a maximum of 1.4 cm³ K mol⁻¹ at 10 K. At 2 K $\chi_m T = 0.4$ cm³ K mol⁻¹. This behavior is observed on both cooling and warming, and is perfectly reproducible. The most likely explanation is the occurrence of a phase transition around 14 K, but, unfortunately, we do not know which molecular rearrangements are involved.

Above 20 K, the magnetic data suggest an antiferromagnetic interaction between the localized spins of $S_{Ni^{III}} = 1/2$ and $S_{Ni^{II}} = 1$. Under this hypothesis, the spin Hamiltonian may be written as in Equation (1), where the first term on the right-hand side describes the isotropic interaction, the second term

$$\mathcal{H} = -J\mathbf{S}_{Ni^{II}} \cdot \mathbf{S}_{Ni^{III}} + D_{Ni^{II}} \cdot \mathbf{S}_{Ni^{II},z^2} + g\beta(\mathbf{S}_{Ni^{II}} + \mathbf{S}_{Ni^{III}}) \cdot \mathbf{H} \quad (1)$$

the local anisotropy (zero-field splitting) of the Ni^{II} ion, and the third term the Zeeman perturbation. With the assumption that the axial zero-field splitting parameter of the Ni^{II} ion has the same value as in nickelocene (i.e. $D_{Ni^{II}} = 25$ cm⁻¹),[12] it is possible to reproduce the magnetic data from the Hamiltonian [Eq. (1)] with $J = -11.8$ cm⁻¹ and $g = 1.98$.

NMR spectroscopy and reactivity: The ¹H NMR spectra for $[Co'Co']^+$, $[Ni'Ni']^{2+}$, and $[Ni'Ni']^+$ are depicted in Figure 3. In all cases the methyl groups of Cp* were identified by their signal areas, while the signals of H2/5 and H3/4 were
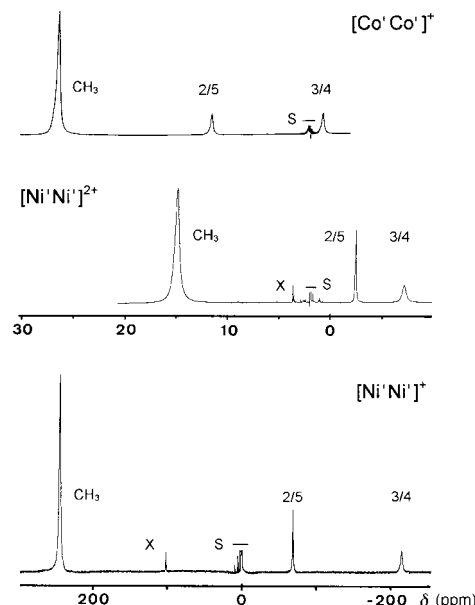

Figure 3. ¹H NMR spectra of $[Co'Co']^+[PF_6]^-$ in CD₃CN, and of $[Ni'Ni']^{2+}[PF_6]_2^-$ and $[Ni'Ni']^+[PF_6]^-$, both in [D₆]acetone. Temperature = 305 K, X = impurity ($[Cp_2^*Ni]^+$), S = solvent. For signal numbering see Scheme 1.

distinguished by determining which molecular orbitals (MOs) carry the spin (see Discussion). Conversion of the experimental signal shifts (δ^{exp}) into the paramagnetic signal shifts at standard temperature, $T = 298$ K (δ^{para}), gave the data collected in Table 1. These values reflect the pure effect of the

Table 1. Paramagnetic ^{1}H and ^{13}C NMR signal data[a] of the cationic decamethylbimetallocenes [Co′Co′]+, [Ni′Ni′]+, and [Ni′Ni′]²+ at 298 K.

Nuclei[b]	[Co′Co′]+[c]	[Ni′Ni′]+[d]	[Ni′Ni′]²+[d]
H2/5	6.3 (90)	−73.9 (320)	−8.1 (30)
H3/4	−4.1 (90)	−223 (810)	−12.1 (100)
CH_3(Cp*)	25.3 (100)	248 (680)	11.8 (120)
C1	312[e]	648[h]	53.9 (150)
C2/5	−51.2[f] (120)	−48[i] (400)	88 (380)
C3/4	255 (450)	644 (1000)	52.9[j] (190)
CCH$_3$(Cp*)	310 (950)	1305 (3200)	78.9 (380)
CCH$_3$(Cp*)	−106.5[g] (120)	−679 (500)	−35.1[k] (150)

[a] Signal shifts δ^{para} relative to corresponding diamagnetic compounds (see Experimental Part); signal half widths in Hz at 305 K in parentheses. [b] For numbering see Scheme 1. [c] Solvent CD$_3$CN. [d] Solvent [D$_6$]acetone. [e] Signal coincides with that of CCH$_3$(Cp*). [f] Doublet, ^1J(C,H) = 120 Hz. [g] Quartet, ^1J(C,H) = 120 Hz. [h] Shoulder. [i] Solvent 1,2-difluorobenzene. [j] Doublet, ^1J(C, H) = 187 Hz. [k] Quartet, ^1J(C,H) = 123 Hz.

unpaired electrons on the nuclei, which is essential to the Discussion. In addition, the signal half-widths (W) are given in Table 1. Note that for [Co′Co′]+ and [Ni′Ni′]²+, W is small enough to allow observation of one-bond C,H couplings [^1J(C,H)].

However, the ^{13}C NMR spectra reproduced in Figure 4 do not show the C,H couplings in every case, for at least one of the engaged nuclei relaxes too rapidly. An example is C3/4 of [Co′Co′]+. While W(H3/4) would be sufficiently small for observable coupling, W(C3/4) indicates fast relaxation which, in fact, causes decoupling. The doublets observed in Figure 5c are rare examples of resolved ^1J(C,H) splittings of Cp carbon

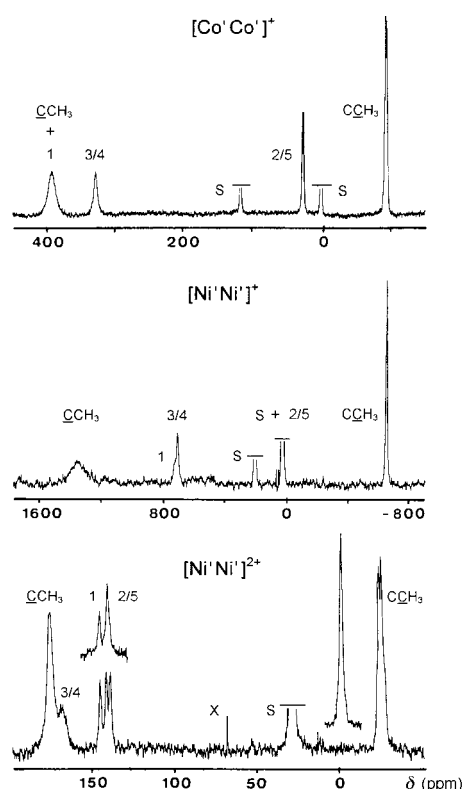Figure 4. ^{13}C NMR spectra of [Co′Co′]+[PF$_6$]− in CD$_3$CN, and of [Ni′Ni′]+[PF$_6$]− and [Ni′Ni′]²+[PF$_6$]$_2^−$ both in [D$_6$]acetone. Temperature = 305 K, X = impurity, S = solvent. For signal numbering see Scheme 1. The insets given for [Ni′Ni′]²+ are the proton-decoupled spectra.

resonances. The only other known instance where paramagnetic d-metal Cp compounds show such a splitting occurs in the μ-alkylidene compound [{CpCr(μ-Cl)}$_2$(μ-CHSiMe$_3$)].[13] The multiplet structure of the signals greatly facilitates assignment, which is aided further by the signal areas. As in the ^{1}H NMR spectra, assignment of the ^{13}C NMR signals for the nuclei in positions 2/5 and 3/4 is based on the MO arguments given below.

Some difficulties were encountered with C1 of [Co′Co′]+. Since the area of the signals assigned to C2/5 and C3/4 was approximately 1:1, and since only four signals could be identified in the range up to 1000 ppm, we were forced to assume that the signals of C1 and C1-5 of Cp* coincided. Temperature-dependent spectra in the range 235–350 K gave no observable signal splitting. When δ^{exp}(C1) and δ^{exp}(CCH$_3$) are equal the referencing procedure yields δ^{para}(C1) = 312 and δ^{para}(CCH$_3$) = 310 (Table 1). Application of the Curie law with back-referencing produces a signal splitting of 2 ppm at best, which cannot be observed owing to the large line width W(CCH$_3$). A similar case in which the signals of C3/4 and CCH$_3$ overlap is that of [Ni′Ni′]²+ (Figure 4), where the signals are just separated, partly because W(CCH$_3$) is sufficently small. As for [Ni′Ni′]+, Figure 4 shows that the signal for C2/5 is hidden under one of the solvent signals. C2/5 could be revealed by recording the spectrum of [Ni′Ni′]+ in 1,2-difluorobenzene.

[Ni′Ni′]²+ slowly decomposed in acetone at 25 °C. Amongst other reaction products, [Ni′Ni′]+ and [Cp*$_2$Ni]+ (δ^{exp} = 103 at 305 K) were identified by their ^{1}H NMR signals. When pure [Ni′Ni′]+ was left in acetone at 25 °C for three months it was converted partly to [Cp*$_2$Ni]+ and also to other unidentified paramagnetic [Cp*Ni] derivatives.

[Co′Co′]+ dissolved in CD$_3$CN underwent selective deuteration of the Cp* ligands that was complete after six months at 25 °C, as substantiated by its ^{1}H NMR spectrum (Figure 5). The CH$_3$ signal in the initial spectrum (Figure 3) disappeared, while the signals of H2/5 and H3/4 were unchanged (Figure 5b). This was verified by the ^{2}H NMR spectrum (Figure 5a) which showed the CD$_3$ resonance with no indication that the fulvalene ligand had been deuterated. As expected, the widths of the corresponding ^{2}H and ^{1}H NMR signals were different (5 and 100 Hz, respectively), although the theoretical factor of 42.4 was not attained.[14] Further evidence for this process was provided by ^{13}C NMR spectroscopy. The quartet of the CH$_3$ group disappeared going from [Co′Co′]+ (Figure 5c) to [D$_{30}$][Co′Co′]+ (Figure 5d) because the smaller coupling ^1J(C,D) (by a factor of 6.5) was not resolved. In contrast, the doublet of C2/5 remained unchanged. We assume that deuteration proceeds in a similar way to that found for alkylated cobaltocenium ions.[15]

Discussion

The new cations [Co′Co′]+ and [Ni′Ni′]+ are mixed-valence species having d^6,d^7- and d^7,d^8-electron counts, respectively. While these species may be formally unsymmetric, their NMR spectra showed only one set of signals for both metallocene fragments. It follows that [Co′Co′]+ and [Ni′Ni′]+ are average-
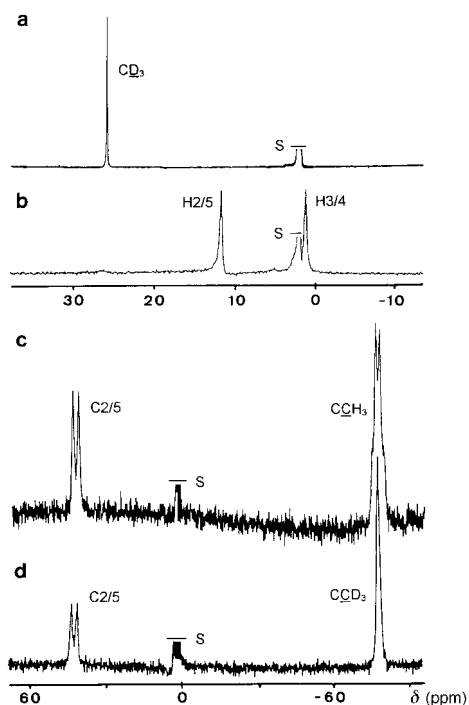
Figure 5. NMR spectra demonstrating the selective deuteration of the Cp* ligands of [Co'Co']+: a) ^{2}H and b) ^{1}H NMR spectra of [D$_{30}$][Co'Co']+ in CH$_3$CN/CD$_3$CN and in CD$_3$CN, respectively ($T = 305$ K). Relevant parts of the ^{13}C NMR spectra of: c) [Co'Co']+ and d) [D$_{30}$][Co'Co']+ in CD$_3$CN at $T = 352$ K. S = solvent. (For signal numbering see Scheme 1.)

valent ions (delocalized or class III in the Robin and Day classification[16]) in the frequency window accessible to NMR spectroscopy. In a temperature-dependency study no signal splitting was observed for [Co'Co']+ down to 235 K. In contrast, investigations of magnetism reveal that solid [Ni'Ni']+[PF$_6$]$^-$ has localized valencies (class I mixed-valence compound).

In order to estimate the frequency and the barrier of the ET we assume that the NMR signal shifts for each half of the valence-localized [Co'Co']+ can be approximated by those of [Co'Co'] and [Co'Co']$^{2+}$[17], and that the corresponding signals of H2/5 ($\delta = -56.8$ and 5.55, respectively)[8] coalesce at 235 K. Simple calculations[18] then yield an ET rate of 4.3×10^4 s^{-1} and a barrier of 36.3 kJ mol^{-1}. Clearly, the actual ET rate of [Co'Co']+ in CD$_3$CN must be higher and the barrier lower. For [Ni'Ni']+ the ET rate exceeds 5.6×10^4 s^{-1} with a barrier lower than 27.4 kJ mol^{-1} at 183 K in (CD$_3$)$_2$CO.[19] [Fe'Fe']+ is another member of the series under discussion. Mössbauer spectroscopy has shown that the salts [Fe'Fe']+[PF$_6$]$^{-[11a]}$ and [Fe'Fe']+[I$_3$]$^{-[11b]}$ are localized mixed-valence compounds in the solid state. Localization in [Fe'Fe']+[I$_3$]$^-$ has also been indicated by the results of X-ray and IR investigations.[11b, c] Whether mixed-valence compounds appear delocalized or localized depends on the frequency window of the physical method employed[20] and also on whether they are studied in solution or in the solid state. Even the nature of the counterion may be important.[4] Therefore, further investigations of the [M'M']+ series would be of interest.

Spin-carrying MOs: If the number of unpaired electrons alone is counted, then the magnetic behavior and the NMR results

obtained are surprising. For instance, [Ni'Ni']$^{2+}$ is antiferromagnetically coupled down to 14 K, whereas [Co'Co'] is ferromagnetically coupled,[8] although both are d^7,d^7 species. Furthermore, the ^{13}C NMR signal pattern of the fulvalene bridge is 1/2/2 for [Ni'Ni']+ (with decreasing shift, see Figure 4), whereas it is 2/1/2 for [Ni'Ni']$^{2+}$ and 2/2/1 for [Co'Co'].[8] This may be understood by consideration of the spin-carrying MOs.

For this purpose we have previously employed the known correlation between the squared carbon 2p$_z$ AO coefficient (c_i^2) of ligand π orbitals and the ^{1}H and ^{13}C NMR contact shifts (δ^{con}).[8] Originally, these correlations were established for the hyperfine coupling constants ($A(^1$H)[21] and $A(^{13}$C)[22]) of organic radicals. For the NMR data of paramagnetic π complexes, we make use of the proportionality $A \propto \delta^{con}$, and we must consider the fact that the ligand π orbitals do not entirely accommodate the unpaired electron. It is, in fact, only partly delocalized on the ligands which are, therefore, treated as reduced-spin radicals by normalization of the calculated c_i^2 before comparison with the normalized δ^{con} values. The latter are obtained after subtraction of the dipolar shifts (δ^{dip}) from δ^{para}. These calculations show that the δ^{dip} values are negligibly small, except for the proton result of [Co'Co']+ (see Experimental Section).

Extended Hückel calculations were performed for [M'M']$^{n+}$ in order to interpret qualitatively the experimental results. At this level of approximation, four MOs must be considered for accommodating the unpaired electrons. Their energy splitting is small, and they are well separated from the next lower doubly occupied MO. The bridging-ligand content of these MOs is shown in Figure 6, where they are labelled with
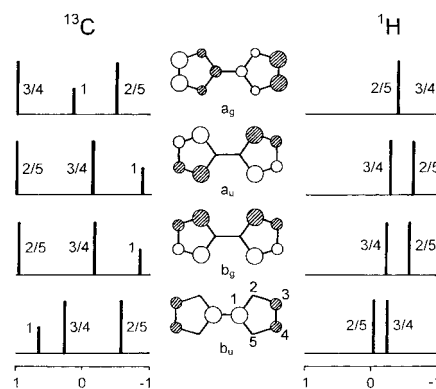

Figure 6. Normalized theoretical ^{13}C and ^{1}H NMR signal patterns obtained from extended Hückel results of [Ni'Ni']$^{2+}$. The patterns shown are those expected for the fulvalene bridge when spin is transmitted selectively to the b_u, b_g, a_u, and a_g orbitals, respectively (see text). From top to bottom the MO energies decrease nonlinearly.[23]

increasing energy: b_u, b_g, a_u, and a_g. For each of these MOs the c_i^2 values were converted[21, 22] into normalized NMR signal shifts, which are also depicted in Figure 6. Note that for a_u and b_g the result is rather similar. In fact, in the fulvalene dianion these orbitals are degenerate, but bonding to Cp*M fragments produces a small splitting.

For comparison, the normalized experimental results (δ^{con} values) are given in Figure 7, together with data obtained
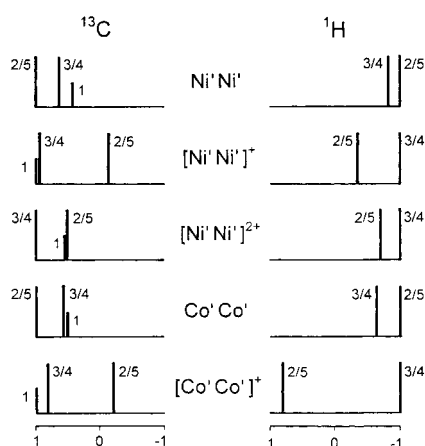
Figure 7. Normalized experimental ^{13}C and ^1H NMR results (contact shifts) for the fulvalene bridge of the cationic decamethylbimetallocenes compared to those of the neutral congeners.[8]

previously.[8] An instructive example is [Ni'Ni']²⁺ which has two magnetically interacting unpaired electrons, and is formally a d⁷,d⁷ species like [Co'Co']. However, the NMR data (Figures 3 and 4, Table 1 and ref. [8]) are rather different. Thus, the smaller ^1H and ^{13}C NMR signal shifts of [Ni'Ni']²⁺ reflect the antiferromagnetic interaction, but [Co'Co'] has a triplet ground state. Even if the magnetic interaction is eliminated artificially by normalization of the data, the signal patterns of [Ni'Ni']²⁺ and [Co'Co'] still differ (Figure 7).

When the patterns for [Ni'Ni']²⁺ are compared with the calculated patterns of Figure 6 it is evident that spin in a single MO cannot explain the results. The agreement should improve when more than one MO contributes to the spin distribution, and according to the MO energies the b_g and a_u orbitals (almost degenerate) should be involved as well as b_u. Model calculations (Figure 8b) show that good agreement with the experimental ^{13}C NMR pattern (Figure 7) is obtained
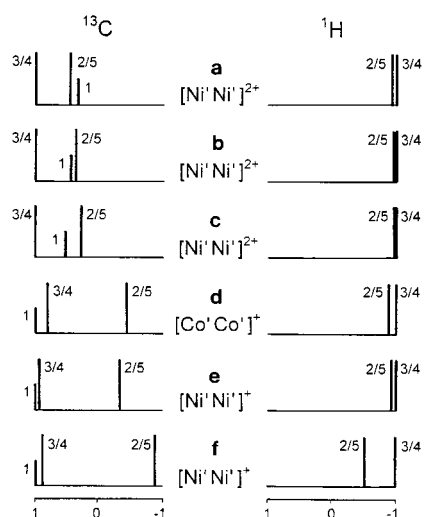

Figure 8. Calculated ^{13}C and ^1H NMR signal patterns for the fulvalene bridge of [M'M']$^{n+}$ arising from spin in more than one of the orbitals shown in Figure 6: [Ni'Ni']²⁺ a)–c) illustrate the dependence of the patterns on the factor $b_u/0.5(b_g + a_u)$ (1.50, 1.53, and 1.56, respectively). [Co'Co']⁺ d) where $b_u/0.5(b_g + a_u) = 1.78$. [Ni'Ni']⁺ e) $b_u/0.5(b_g + a_u) = 1.82$; f) $b_u/0.5(b_g + a_u)/a_g = 4/1/1.7$.

when b_u and $b_g + a_u$ contribute 60.5% and 39.5%, respectively. As the traces of Figure 8a–c demonstrate, the ^{13}C NMR pattern is rather sensitive to changes in the orbital contributions. However, a perfect agreement between experimental and calculated patterns would be coincidental, as a) the EHMO approach is crude, b) the geometry of the ion must be estimated (see Experimental Section), and c) the fourth MO (a_g) may be slightly populated (see below). In addition, when the signal shifts are small, the dipolar contributions cause some ambiguity as they depend on the g factor anisotropy, and only a range of g factors, rather than precise values, is known in some cases. This explains why the experimental and calculated ^1H patterns deviate.

Assignment of the NMR signals requires only qualitative treatment of these results. Figure 8 shows that the signals for C3/4 and H3/4 of the fulvalene bridge in [Ni'Ni']²⁺ are shifted more than those for C2/5 and H2/5. Rather unexpectedly, this is the reverse of the signal sequences for [Co'Co'] (Figure 7). This example and those that follow demonstrate that model calculations are the surest way to assign NMR signals for this sort of fulvalene complex.

The simplest case is [Co'Co']⁺. It has one unpaired electron, which would be expected to reside in the b_u orbital. In fact, the experimental ^{13}C NMR signal pattern (Figure 7) is similar to that calculated for the spin in the relevant b_u orbital of [Co'Co']⁺, and this, in turn, bears similarity to that of the b_u orbital of [Ni'Ni']²⁺ in Figure 6. However, the agreement between theory and experiment may be improved by allowing the b_g and a_u orbitals to be populated in addition to b_u (Figure 8). This situation arises with [Ni'Ni']²⁺, and it agrees with the fact that the EHMO energies change very little in the [M'M']$^{n+}$ series.[23] As in the case of [Ni'Ni']²⁺, the simulated ^1H NMR data are poorer than the ^{13}C data.

The product $\chi_m T$ for [Co'Co']⁺ at ambient temperature is about half that for [Co'Co']. This is reflected in the ^1H and ^{13}C NMR signal shifts of the Cp* ligand which are smaller for [Co'Co']⁺ than for [Co'Co'] (Table 1 and ref. [8]). However, the mean factor is 0.63 rather than 0.5. We conclude, therefore, that the metal-to-ligand spin transfer in [Co'Co']⁺ is more efficient than in [Co'Co'].

For [Ni'Ni']⁺ the NMR signal shifts are caused by three unpaired electrons. If the signal shifts are considered to be proportional to $S(S+1)$, and the contributions of $S=1$ and $S=\frac{1}{2}$ are averaged, then a rough comparison with nickelocenes may be made. Consequently, these shifts should be almost 70% of those found for the nickelocenes;[24] that is, for the probe Cp* approximately 1030 ppm (CCH_3), −460 ppm (CCH_3m), and 170 ppm (CCH_3). These values are smaller than are observed for [Ni'Ni']⁺ (Table 1). This suggests that the spin delocalization in [Ni'Ni']⁺ is more efficient than in nickelocenes, which is in line with the properties of [Co'Co']⁺.

The ^{13}C NMR signal pattern of the fulvalene bridge of [Ni'Ni']⁺ could be well reproduced by considering spin to be once more in the orbitals b_u, b_g, and a_u (Figures 6, 7, and 8). In contrast, the corresponding calculated ^1H NMR pattern deviated similarly to that of [Co'Co']⁺ and [Ni'Ni']²⁺. These last two cations have small signal shifts for the nuclei of the fulvalene bridge, which could be perturbed by small dipolar shifts. This does not apply to [Ni'Ni']⁺, which has much larger

proton signal shifts (Table 1). We have therefore tried to improve the calculated NMR signal pattern by admixing some a_g orbital contribution. Although this is demonstrated successfully in Figure 8f, we consider it to be tentative, as the number of adjustable parameters at the given level of approximation is a serious limitation. For all the cations $[M'M']^{n+}$ an inverted assignment of C2/5 and C3/4 was tested. In these cases either it was completely impossible to reproduce the experimental signal sequence, or the agreement between theory and experiment was much worse.

Magnetic interaction: We have previously suggested that the ferromagnetic interaction in $[Co'Co']$ arises from the accidental degeneracy of the orbitals.[8] In fact, the MO calculations show that throughout the series $[M'M']^{n+}$ the relevant orbitals b_u, b_g, a_u, and a_g are close in energy.[23] It follows that slight modifications of $[M'M']^{n+}$ will lead to orbital degeneracies or remove them, and that they will thus influence strongly the magnetic behavior. Such changes include variation of M, of the external charge, of the number of unpaired electrons, of the ligand substituents, and of the metal-to-ligand distance. This idea is substantiated by the fact that the d^7,d^7 species $[Co'Co']$ and $[Ni'Ni']^{2+}$ are ferro- and antiferromagnetic, respectively. Further modifications of the d^7,d^7 bimetallocenes must show how robust the triplet ground state actually is.

It is also possible to attribute the magnetism of the compounds $[M'M']^{n+}$ to the interaction between the metallocene units. As discussed in earlier work,[8] the interaction is essentially mediated by the bridging fulvalene ligand, because the metal–metal distance is large (>520 pm). The relevant parts of the π orbitals which may carry the spin are shown in Figure 6. The b_u and a_g orbitals have a big AO coefficient at the carbon atoms that join the two five-membered rings (C1 and C1'), and hence the antiferromagnetic interaction will be strong. In contrast, it will be much smaller for the b_g and a_u orbitals so that ferromagnetic interaction can dominate. There are gross factors that determine the overall magnetic interaction, one of which is the amount of spin transferred to each MO (hence the interest in determining the spin distribution). The second factor concerns the interactions between the orbitals of the two five-membered rings which are not restricted to the $2p_z$ AOs of C1 and C1'.[8]

The propensity of $[M'M']^{n+}$ to change the magnetic behavior is also reflected in the J values, which are similar for $[Ni'Ni']^{2+}$ (-240 cm^{-1}) and $Ni'Ni'$ (-180 cm^{-1}),[8] while J drops to -11.8 cm^{-1} for $[Ni'Ni']^+$. Yet another indication is the magnetic phase transition of $[Ni'Ni']^+[PF_6]^-$ at 14 K (Figure 2). The relevance of the magnetic data below 20 K is not clear. However, we observe that the $\chi_m T$ value at 10 K seems to be larger than the paramagnetic limit. This suggests that below the temperature of the phase transition some ferromagnetic interactions are operative. If these ferromagnetic interactions were intramolecular, the ground state spin for $[Ni'Ni']^+$ would be $S = ^3/_2$, and the magnetic data below 10 K might arise from the zero-field splitting of this $S = ^3/_2$ state. Without any structural information it is not possible to improve the interpretation of the data, but the counterion may also play an important role. Also noteworthy is that for a

fully delocalized $Ni^{II}Ni^{III}$ mixed-valence pair, the $S = ^3/_2$ state is expected to be stabilized strongly through a double-exchange mechanism.[25]

The only other compounds of this sort studied so far by magnetic measurements are $[FeFe]^{2+}[BF_4]_2^-$ [10b] and $[Fe'Fe']^{2+}[I_3]_2^-$.[11b] No magnetic interaction was considered for the interpretation of the data of $[FeFe]^{2+}$, while the magnetic susceptibility of $[Fe'Fe']^{2+}$ was seen to follow the Curie–Weiss law with a Weiss constant of $\theta = -5.58$ K.

Conclusion

Electron transfer potentials have again proven to be a valuable guide in isolating mixed-valence species. The decamethylmetallocenium cations $[Co'Co']^+$ and $[Ni'Ni']^+$ were obtained from $[Ni'Ni']$ and $[Co'Co']^{2+}$ by simple redox reactions. Further oxidation of $[Ni'Ni']^+$ gave $[Ni'Ni']^{2+}$.

The species $[M'M']^{n+}$ may be regarded simply as the product of metallocene coupling, but some new properties have been found. In particular, the resulting compound acts as a 'magnetic chameleon' when more than one unpaired electron is present. In a previous study,[8] weak and strong antiferromagnetic interactions were found for $[V'V']$ and $[Ni'Ni']$, respectively, whereas the d^7,d^7 compound $[Co'Co']$ is strongly ferromagnetic. $[Ni'Ni']^{2+}$, described in this work, is a d^7,d^7 analogue, which experiences strong antiferromagnetic interaction, whereas $[Ni'Ni']^+$ shows weak antiferromagnetic coupling, but seems to become ferromagnetic below 14 K.

MO analysis of the Co and Ni derivatives showed that such behavior results from the near degeneracy of four orbitals whose splitting is sensitive both to the nature of the metal and to the charge of $[M'M']^{n+}$. It was possible to probe the ligand contribution of these MOs by NMR spectroscopy which, in turn, established the metal-to-ligand spin transfer. The NMR signals for the nuclei of the fulvalene bridge can be understood if more than one π orbital accommodates spin and so these orbitals must be involved in the magnetic interaction. The signal shifts of the Cp* ligand are a measure of the overall spin transfer, which is more efficient for the cations $[M'M']^{n+}$ than for the neutral compounds $[M'M']$.

Experimental Section

Decamethylbinickelocenium(II,III) bis(hexafluorophosphate)
([Ni′Ni′]²⁺[PF₆]₂⁻): [Ni′Ni′][8] (330 mg, 0.64 mmol) was dissolved in THF (150 mL), and [Cp₂*Fe]⁺[PF₆]⁻ (600 mg, 1.27 mmol) was added with stirring at 25 °C. The reaction was accompanied by a color change from deep red-violet to dark green. The solvent was removed in vacuo, and hexane (50 mL portions) was used to extract [Cp₂*Fe] from the residue. The remaining powder was recrystallized twice from acetone to yield the green [Ni′Ni′]²⁺[PF₆]₂⁻ (390 mg, 76 %). CV ($E_{1/2}$, mV vs. [Cp₂Fe]/[Cp₂Fe]⁺ [ΔE_p, mV; $i_\mathrm{pa}/i_\mathrm{pc}$]): −640 [65; obscured by impurity] ([Ni′Ni′]⁺/[Ni′Ni′]²⁺); 150 [78; 1.03] ([Ni′Ni′]²⁺/[Ni′Ni′]³⁺); 625 [195; obscured by solvent] ([Ni′Ni′]³⁺/[Ni′Ni′]⁴⁺); C₃₀H₃₈F₁₂Ni₂P₂ (806.0): calcd C 44.71, H 4.75, Ni 14.57, F 28.28, P 7.69; found C 44.21, H 4.63, Ni 14.17, F 27.65, P 7.75.

Decamethylbicobaltocenium(II,III) hexafluorophosphate ([CoCo]⁺[PF₆]⁻): Sodium amalgam (5.47 g, 1.94 % Na, 4.63 mmol) was added to a suspension of [Co′Co′]²⁺[PF₆]₂⁻[8] (3.39 g, 4.20 mmol) in THF (200 mL). The mixture was stirred for 3 days to produce a color change from yellow to green, after which a light green solid was obtained by filtration. The solid was washed twice with hexane (50 mL portions). Recrystallization from acetonitrile yielded dark green crystals of [Co′Co′]⁺[PF₆]⁻ (2.43 g, 97 %). CV ($E_{1/2}$, mV vs. [Cp₂Fe]/[Cp₂Fe]⁺ [ΔE_p, mV; $i_\mathrm{pa}/i_\mathrm{pc}$]): −1370 [90; 1.08] ([Co′Co′]²⁺/[Co′Co′]⁺); −1800 [80; 0.99] ([Co′Co′]⁺/[Co′Co′]); −2655 [130; 1.03] ([Co′Co′]/[Co′Co′]⁻); −3150 [170; 1.05] ([Co′Co′]⁻/[Co′Co′]²⁻); C₃₀H₃₈Co₂P₆F (661.5): calcd C 54.47, H 5.79, Co 17.82, F 17.23, P 4.68; found: C 54.42, H 5.82, Co 17.10, F 17.95, P 5.01.

Physical measurements: The CVs were obtained with equipment described previously.[26] The samples were dissolved in solutions of *n*Bu₄NPF₆ in propionitrile (0.1 M) at −21 °C. The solvent was dried by passing it over activated Al₂O₃ placed in a tube within the cell. The concentrations were 2.5×10^{-4} and 9.7×10^{-4} mol L⁻¹ for [Co′Co′] and [Ni′Ni′], respectively. The scan rate was 200 mV s⁻¹. [Cp₂Co]⁺[PF₆]⁻ and [Cp₂Fe] were added as internal standards for [Ni′Ni] and [Co′Co′], respectively. The CV data of the mixed sandwiches [Cp*MCp] were needed for comparison and are summarized in Table 2.

Table 2. Electrochemical data[a] for pentamethylmetallocenes.

	[Cp*FeCp]	[Cp*CoCp]	[Cp*NiCp]
$E_{1/2}$ (−1/0)[b]		−2755	−2450[c]
ΔE_p (−1/0)		125	[c]
$E_{1/2}$ (0/1)	−265	−1655	−850
$\Delta E_{1/2}$ (0/1)	62	60	65
$i_\mathrm{pc}/i_\mathrm{pa}$ (0/1)	[d]	1.3	1.1
$E_{1/2}$ (1/2)			120
ΔE_p (1/2)			80
$i_\mathrm{pc}/i_\mathrm{pa}$ (1/2)			0.8

[a] In propionitrile at 20 °C except for [Cp*CoCp] (−20 °C); concentration 0.8 mm, 1.5 mm, and 2.8 mm, for the Fe, Co, and Ni derivative, respectively; supporting electrolyte 0.1 M *n*Bu₄NPF₆; scan rate 200 mV s⁻¹. Potentials in mV relative to [Cp₂Fe]/[Cp₂Fe]⁺. [b] The external charges of the involved species are given in parentheses. [c] Anodic wave of an irreversible electron transfer. [d] Disturbed by a trace of [Cp₂Fe].

The NMR spectra were recorded on Bruker CXP 200, Bruker MSL 300, JEOL JNM GX 270 spectrometers with samples held in standard tubes equipped with ground glass and stoppers (¹H NMR), and with solenoid tubes[27] (¹³C NMR). The temperature was calibrated with a Pt resistance thermometer placed in a tube which contained ethylene glycol. Experimental signal shifts δ^exp were measured relative to solvent peaks. In order to obtain the paramagnetic signal shifts at the temperature of measurement T, the δ^exp values of [Ni′Ni′]²⁺ were calculated relative to the signal shifts of [Co′Co′]²⁺,[8] and the δ^exp values of [Ni′Ni′]⁺ and [Co′Co′]⁺ were calculated relative to the mean of the signal shifts of [Fe′Fe′][8] and [Co′Co′]²⁺. The standard shifts at 298 K (δ^para) were estimated from temperature-dependent ¹H NMR measurements. The ¹³C NMR spectra were recorded at less than 10 K above 298 K, and the δ^para values were obtained under the assumption that the Curie law holds in the narrow temperature range.

The dipolar NMR signal shifts (δ^dip) at 298 K were estimated in line with the work of Kurland and McGarvey.[28] Standard distances (C−H = 1.1,

C−C = 1.42, C−CH₃ = 1.50 Å) were used for the ligands to obtain the geometric factor. The metal-to-ligand distances were those given by the extended Hückel calculation below. The g factors were allowed to vary:[29] $g_\parallel = 1.721$–1.707, $g_\perp = 1.772$–1.854 for cobaltocene fragments, and $g_\parallel = 1.768$–1.878, $g_\perp = 1.865$–2.024 for nickelocenium fragments. For the nickelocene fragment $g_\parallel = 2.003$, $g_\perp = 2.09$,[12] and a zero field splitting of $D = 25$ cm⁻¹[12] was used. These values were inserted into Equation 2 to

$$\delta^\mathrm{dip} = \frac{\mu_\mathrm{o}}{4\pi} \frac{\beta^2 S(S+1)}{9kT} \frac{3\cos^2\phi - 1}{r^3} (g_\parallel^2 - g_\perp^2) \cdot \left[1 - \frac{g_\parallel^2 + 0.5 g_\perp^2}{3(g_\parallel^2 - g_\perp^2)} Dk^{-1}T^{-1}\right] \quad (2)$$

give the values shown in Table 3. (μ_o = permeability of vacuum, β = Bohr magneton, k = Boltzmann constant, T = absolute temperature, r = vector relating the metal and the nucleus under study, φ = angle between r and the ligand–metal–ligand axis of the metallocene fragment, g = electron g factor, and D = zero field splitting.) Subtraction of δ^dip from δ^para (Table 1) yielded δ^con, also listed in Table 3.

Table 3. ¹H and ¹³C dipolar (δ^dip) and contact (δ^con) shifts[a] of the cationic decamethylbimetallocenes [Co′Co′]⁺, [Ni′Ni′]⁺, and [Ni′Ni′]²⁺ at 298 K.

Nuclei[b]	[Co′Co′]⁺		[Ni′Ni′]⁺		[Ni′Ni′]²⁺	
	δ^dip	δ^con	δ^dip	δ^con	δ^dip	δ^con
H2/5	−1.6	7.9	−8.0	−65.9	−1.8	−6.3
H3/4	−1.6	−2.5	−8.0	−215	−1.8	−10.3
CCH₃	−0.4	27.5	−2.3	250	−0.5	12.3
C1	−7.6	320	−22.6	671	−8.0	61.9
C2/5	−7.0	−44.2	−33.2	−15	−6.8	95
C3/4	−7.0	262	−33.2	677	−6.8	59.7
CCH₃	−6.9	317	−32.7	1338	−6.9	85.8
CCH₃	−0.4	−106.1	−4.8	−674	−0.5	−34.6

[a] Values obtained from maximal g-factor anisotropy. [b] For numbering see Scheme 1.

The magnetic measurements were performed with a SQUID magnetometer at temperatures between 1.7 and 300 K. The samples were sealed in quartz tubes under vacuum. The data were corrected for the magnetization of the sample holders and for the core diamagnetism.

Extended Hückel calculations: The program devised by Mealli and Prosperio[30] (Version 4.0, 1994) was used for these calculations. Idealized structures for the decamethylmetallocenium ions were assumed, and the bond lengths were adapted from those of [Cp₂M] (M = Fe, Co, Ni),[31] [Fe′Fe′],[11a] and [Fe′Fe′]⁺[I₃]⁻.[11b] When these last two structures were compared to that of [Cp₂Fe] they showed characteristic differences in the metal-to-ligand distances which depended on whether the fulvalene (fv) or the Cp* ligand was concerned (M−fv and M−Cp*, respectively). These distances also depended on charge. For the ions [M′M′]⁺ in this work, M−fv and M−Cp* were obtained from [Cp₂M], taking into account the changes in passing from [Cp₂Fe] to [Fe′Fe′]⁺, that is, [Co′Co′]⁺ (delocalized) M−fv = 1.757 Å and M−Cp* = 1.774 Å; [Ni′Ni′]⁺ (delocalized) M−fv = 1.854 Å and M−Cp* = 1.873 Å; and [Ni′Ni′]²⁺ M−fv = 1.870 Å and M−Cp* = 1.886 Å.

Acknowledgments

[1] D. Astruc, *Electron Transfer and Radical Processes in Transition Metal Chemistry*. VCH, Weinheim, **1995**.

[2] D. Astruc, *Acc. Chem. Res.* **1997**, *30*, 383–391.

[3] S. Barlow, D. O'Hare, *Chem. Rev.* **1997**, *97*, 637–669.

[4] a) R. J. Webb, S. J. Geib, D. L. Staley, A. L. Rheingold, D. N. Hendrickson, *J. Am. Chem. Soc.* **1990**, *112*, 5031–5042; b) T.-Y. Dong, S. H. Lee, T. Y. Lee, *Organometallics* **1996**, *15*, 2354–2359.

[5] a) G. E. McManis, R. M. Nielson, M. J. Weaver, *Inorg. Chem.* **1988**, *27*, 1827 – 1829; b) H. Schottenberger, G. Ingram, D. Obendorf, R. Tessardi, *Synlett* **1991**, 905 – 907; c) H. Schottenberger, G. Ingram, D. Obendorf, *J. Organomet. Chem.* **1992**, *426*, 109 – 119.

[6] a) P. Hudeczek, Diploma Thesis, Technische Universität München, **1990**; b) P. Hudeczek, F. H. Köhler, *Organometallics* **1992**, *11*, 1773 – 1775.

[7] The prime means that each metallocene moiety has one Cp* (pentamethylcyclopentadienyl) ligand; the non-methylated bimetallocenes are abbreviated to MM.

[8] H. Hilbig, P. Hudeczek, F. H. Köhler, X. Xie, P. Bergerat, O. Kahn, *Inorg. Chem.* **1998**, *37*, 4246 – 4257.

[9] T. Matsumoto, M. Sato, A. Ichimura, *Bull. Chem. Soc. Jpn.* **1971**, *44*, 1720.

[10] a) F. Kaufman, D. O. Cowan, *J. Am. Chem. Soc.* **1970**, *92*, 6198 – 6204; b) D. O. Cowan, G. A. Candela, F. Kaufmann, *J. Am. Chem. Soc.* **1971**, *93*, 3889 – 3893.

[11] a) S. Rittinger, D. Buchholz, M.-H. Delville-Desbois, J. Linarès, F. Varret, R. Boese, L. Zsolnai, G. Huttner, D. Astruc, *Organometallics* **1992**, *11*, 1454 – 1456; b) M.-H. Delville, F. Robert, P. Gouzerh, J. Linarès, K. Boukheddaden, F. Varret, D. Astruc, *J. Organomet. Chem.* **1993**, *451*, C10 – C12; c) M.-H. Delville, S. Rittinger, D. Astruc, *J. Chem. Soc. Chem. Commun.* **1992**, 519 – 520.

[12] S. Li, Y. M. Hamrick, R. J. Van Zee, *J. Am. Chem. Soc.* **1992**, *114*, 4434 – 4436 and references therein.

[13] F. H. Köhler, C. Krüger, H. Zeh, *J. Organomet. Chem.* **1990**, *386*, C13 – C15; H. Zeh, Dissertation, Technische Universität München, **1989**.

[14] N. Hebendanz, F. H. Köhler, F. Scherbaum, B. Schlesinger, *Magn. Reson. Chem.* **1989**, *27*, 798 – 802.

[15] A. N. Nesmeyanov, D. N. Kursanov, E. V. Bykova, E. V. Leonova, V. N. Setkina, N. S. Kochetkova, *Bull. Acad. Sci. USSR Div. Chem. Sci. (Engl. Transl.)* **1978**, *27*, 57 – 60.

[16] M. B. Robin, P. Day, *Adv. Inorg. Chem. Radiochem.* **1967**, *10*, 247 – 422.

[17] Spin delocalization from the paramagnetic to the diamagnetic part of localized [Co′Co′]⁺ is neglected.

[18] J. Sandström, *Dynamic NMR Spectroscopy*, Academic Press, London, **1982**, ch. 6,7.

[19] Localized [Ni′Ni′]⁺ is approximated by [Ni′Ni′] and [Ni′Ni′]²⁺, which have signals for H2/5 at $\delta = -87.7$ and 5.4, respectively, at 183 K.

[20] Ref. [1], ch. 1.3.

[21] R. S. Drago, *Physical Methods in Chemistry*, Saunders, Philadelphia, **1977**, ch. 9; S. Ouishi, I. Nitta, *J. Chem. Phys.* **1963**, *39*, 2848 – 2849.

[22] T. Yonezawa, T. Kawamura, H. Kato, *J. Chem. Phys.* **1969**, *50*, 3482 – 3492.

[23] The energy differences obtained from EHMO calculations are 180 – 211 meV between b_u and b_g, 4 – 7 meV between b_g and a_u, and 246 – 251 meV between a_u and a_g. The metals in [M′M′]$^{n+}$ are Co and Ni, and charges run from 0 to 2 +.

[24] F. H. Köhler, K.-H. Doll, W. Prössdorf, *Angew. Chem.* **1980**, *92*, 487 – 488; *Angew. Chem. Int. Ed. Engl.* **1980**, *19*, 479 – 480; F. H. Köhler, K.-H. Doll, *Z. Naturforsch. Teil B* **1982**, *37*, 144 – 150; F. H. Köhler, W. A. Geike, *J. Organomet. Chem.* **1987**, *328*, 35 – 47.

[25] a) G. Blondin, J. J. Girerd, *Chem. Rev.* **1990**, *90*, 1359 – 1376; b) O. Kahn, *Molecular Magnetism*, VCH, New York, **1993**, ch. 13.

[26] H. Atzkern, J. Hiermeier, F. H. Köhler, A. Steck, *J. Organomet. Chem.* **1991**, *408*, 281 – 296.

[27] F. H. Köhler, B. Metz, W. Strauss, *Inorg. Chem.* **1995**, *34*, 4402 – 4413.

[28] R. J. Kurland, B. R. McGarvey, *J. Magn. Reson.* **1970**, *2*, 286 – 301.

[29] L. Zoller, E. Moser, J. H. Ammeter, *J. Phys. Chem.* **1986**, *90*, 6632 – 6638.

[30] C. Mealli, D. M. Prosperio, *J. Chem. Educ.* **1990**, *67*, 399 – 402.

[31] A. Haaland, *Acc. Chem. Res.* **1979**, *12*, 415 – 422.